



# ***NTRK3-EML4*-rearranged spindle cell tumor with co-expression of S100 and CD34: an unusual mesenchymal tumor in the spectrum of the bland-looking spindle cell lesions of the oral cavity**

Giuseppe Broggi, MD, PhD,<sup>a</sup> Giulio Attanasio, MD,<sup>a</sup> Antonio Bonanno, MD,<sup>b</sup> Ignazio La Mantia, MD,<sup>b</sup> Sabina Barresi, PhD,<sup>c</sup> Rita Alaggio, MD, PhD,<sup>c,d</sup> and Gaetano Magro, MD, PhD<sup>a</sup>

A novel category of spindle cell tumors characterized by *Neurotrophic Tyrosine Receptor Kinase (NTRK)* rearrangements with a dual immunoreactivity for S-100 and CD34 has emerged in the last years as a distinct entity among soft tissue neoplasms. These genetic alterations lead to the continuous activation of *NTRK* genes, driving tumorigenesis and offering a unique prospect for targeted therapy. We herein present a rare case of *NTRK3*-rearranged spindle cell tumor with a hitherto unreported gene fusion involving the exon 14 of *NTRK3* with the exon 2 of *Echinoderm Microtubule-Associated Protein-Like 4*, arising in the head and neck region. Tumor occurred in a 45-year-old patient who presented with a painful nodule in the oral mucosa. Due to the possibility of personalizing the treatment strategy for such tumors, pathologists should be aware of this emerging group of spindle cell tumors to promptly recognize them even when they occur in uncommon locations, including the oral cavity. (Oral Surg Oral Med Oral Pathol Oral Radiol 2024;138:635–640)

*Neurotrophic Tyrosine Receptor Kinase (NTRK)* rearrangements have gained significant attention in recent years due to their implications for tumor diagnosis and treatment.<sup>1,2</sup> Accurate diagnosis of *NTRK* fusion-positive tumors relies on comprehensive molecular profiling techniques, including fluorescence in situ hybridization (FISH), reverse transcriptase-polymerase chain reaction (RT-PCR), and next-generation sequencing (NGS).<sup>3,4</sup>

Fusion events involving kinase genes, leading to the oncogenic activation of various kinase proteins, have been increasingly recognized in mesenchymal tumors.<sup>5</sup> The histologic spectrum of kinase fusion-positive mesenchymal tumors has expanded to encompass several emerging entities, including lipofibromatosis-like neural tumors (LPFNTs), infantile fibrosarcoma (IFS)-like, inflammatory myofibroblastic tumor (IMT)-like as well as malignant peripheral nerve sheath tumor (MPNST)-like.<sup>6-8</sup> It is crucial to be aware of the wide

morphological spectrum of these tumors to confirm the diagnosis by means of immunohistochemical and molecular tests.<sup>9</sup> The detection of the underlying fusions can be potentially exploitable for targeted therapy using various kinase inhibitors.<sup>9</sup>

Most of these lesions exhibit a monotonous proliferation of bland-looking spindle cells, often arranged in a patternless or vaguely fascicular pattern, with deposition of stromal and perivascular keloid-like collagen fibers; occasionally scattered pleomorphic and/or multinucleated cells can be seen.<sup>10,11</sup> Most cases show low cellularity, low mitotic count and absence of tumor necrosis. Although some cases may exhibit an overlapping morphology with LPFNTs, others display distinctive hyalinization and overt malignant histologic features, such as high cellularity, fascicular growth pattern, brisk mitotic activity and a primitive appearance.<sup>10,11</sup> Immunohistochemically, many of these tumors, regardless of the kinase fusion type, exhibit focal to diffuse co-expression of S100 and CD34, while SOX10 is consistently negative.<sup>12</sup> Recognizing the wide histologic spectrum of these tumors is crucial to ask for appropriate immunohistochemistry and molecular testing for detecting the underlying gene rearrangements.<sup>9-12</sup> We herein present a rare case of *NTRK3-Echinoderm Microtubule-Associated Protein-Like 4 (EML4)*-rearranged spindle cell tumor occurring in the oral mucosa of a 54-year-old patient. The pathologic features and differential diagnoses are emphasized and discussed.

<sup>a</sup>Department of Medical, Surgical Sciences and Advanced Technologies “G.F. Ingrassia”, Anatomic Pathology, University of Catania, Catania, Italy.

<sup>b</sup>Department of Medical and Surgical Sciences and Advanced Technologies “GF Ingrassia” ENT Section, University of Catania, Catania, Italy.

<sup>c</sup>Pathology Unit, Bambino Gesù Children’s Hospital IRCCS, Rome, Italy.

<sup>d</sup>Department of Medical-Surgical Sciences and Biotechnologies, Sapienza University of Rome, Polo Pontino, Rome, Italy.

Corresponding author: Giuseppe Broggi. E-mail address: [giuseppe.broggi@gmail.com](mailto:giuseppe.broggi@gmail.com)

Received for publication Feb 5, 2024; returned for revision May 11, 2024; accepted for publication May 17, 2024.

© 2024 The Author(s). Published by Elsevier Inc. This is an open access article under the CC BY license (<http://creativecommons.org/licenses/by/4.0/>)

2212-4403/\$-see front matter

<https://doi.org/10.1016/j.oooo.2024.05.010>

## **CASE PRESENTATION**

A 54-year-old male presented to the Ear Nose and Throat Clinic of our hospital with a history of a slow-growing, painless, sessile mass arising from the maxillary left posterior gingiva (Figure 1A) and measuring

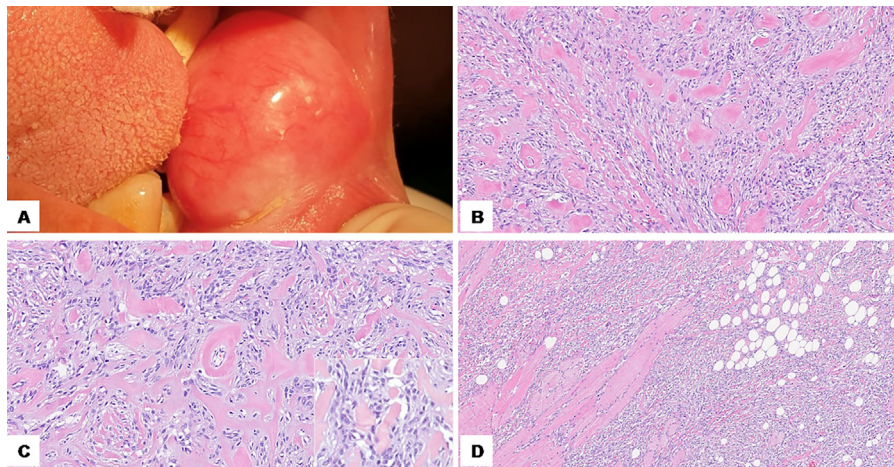


Fig. 1. (A) A slow-growing, painless nodule extending through the vestibule to the buccal mucosa is seen. (B) Low-power magnification showing a monotonous proliferation of bland-looking spindle-shaped cells arranged haphazardly and in short intersecting fascicles (hematoxylin and eosin; original magnification 100 $\times$ ). (C) Neoplastic proliferation is interrupted by numerous thick, keloid-like collagen bands. Perivascular hyalinization is also seen (hematoxylin and eosin; original magnification 200 $\times$ ). Note the mild nuclear atypia of neoplastic cells at higher magnification (insert; original magnification 400 $\times$ ) (D) Diffuse infiltration of the surrounding striated muscle and adipose tissue is shown (hematoxylin and eosin; original magnification 50 $\times$ ).

about 3 cm in its greatest dimension, that had been present for 10 months. The lesion extended from the maxillary gingiva through the vestibule and also involved the buccal mucosa. No history of previous local trauma was reported. The patient had a noncontributory medical and social history. Clinically, the lesion presented as a whitish and infiltrative nodule and firm in consistency. No evidence of bleeding or exudates was seen. Routine panoramic radiography showed the lack of bone resorption. Magnetic resonance imaging studies revealed extensive infiltration of the surrounding musculature and adipose tissue. Accordingly, an excisional biopsy was performed under local anesthesia.

Grossly, the surgical sample consisted of a brownish-white mass of approximately 3  $\times$  2.5  $\times$  1.5 cm in size. The cut surface of the lesion appeared yellowish-white in color and firm in consistency. Tissue specimens were formalin-fixed, paraffin-embedded, cut to 4 microns, and stained with hematoxylin and eosin. Immunohistochemical analyses were performed with the labeled streptavidin-biotin peroxidase detection system using the Ventana automated immunostainer (Ventana Medical Systems, Tucson, AZ, USA). The following antibodies were tested: CD34 (1:50), S100, vimentin (1:100);  $\alpha$ -smooth muscle actin (1:200); desmin (1:100); cytokeratin (CK) AE1/AE3 (1:50); SOX-10 (1:100); MELAN-A (1:200); HMB-45 (1:150); ALK protein (1:50); STAT-6 (1:200); ERG (1:200); CD10 (1:100); EMA (1:200); trimethylated histone 3 at lysine residue 27 (H3K27me3) (1:500); INI-1 (1:200); CD99 (1:100) and HHV-8 (1:50); all from Dako, Glostrup, Denmark.

Histologic examination revealed a monotonous proliferation of bland-looking spindle cells arranged haphazardly (patternless) or in short intersecting fascicles (Figure 1B). This growth pattern was interrupted by several thick keloid-like collagen bands (Figure 1B). Although mild nuclear pleomorphism was focally seen, mitotic count was very low (<1/50 HPFs), and tumor necrosis was absent. The tumor exhibited diffuse infiltration into the surrounding striated muscle and adipose tissue (Figure 1B). Immunohistochemically, neoplastic cells were diffusely and strongly stained with CD34 (Figure 2A), vimentin and S-100 protein (Figure 2B), while no immunoreactivity for SOX-10 (Figure 2C), MELAN-A, HMB-45,  $\alpha$ -smooth muscle actin, desmin, ALK protein, STAT-6, ERG, CKAE1/AE3, CD10, EMA, CD99 and HHV-8 was found. Notably, the neoplastic cells retained INI-1 and H3K27me3 expression.

Differential diagnosis mainly revolved around primary/metastatic melanoma, spindle cell MPNST, reparative keloid tissue, dermatofibroma, myoepithelioma, leiomyoma, and schwannoma. Melanoma was ruled out on the basis of the clinical history of the patient, which was unremarkable for previous melanomas, along with the diffuse CD34 immunoreactivity and the absence of the expression of melanocytic markers (SOX-10, HMB45, Melan A). Unlike the case herein presented, MPNSTs (85%-90% cases) are usually high-grade spindle cell sarcomas with diffuse moderate-to-severe cytological atypia, high mitotic activity, and tumor necrosis. The typical features consisting of hypercellular areas arranged in densely cellular fascicles, often alternating and interdigitating with more hypocellular and myxoid areas, were lacking in our

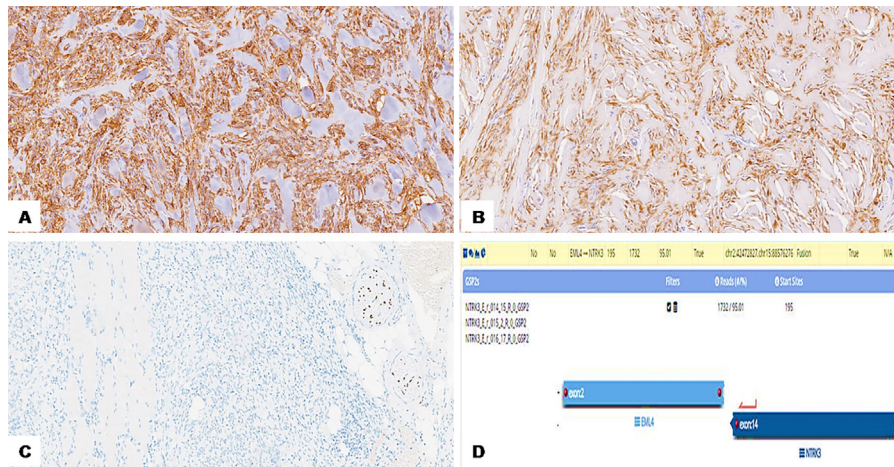


Fig. 2. Neoplastic cells are diffusely and strongly stained with CD34 (A) and S100 protein (B), while they are consistently negative for SOX10 (C) (immunoperoxidase; original magnifications 200×). (D) Illustrative representation of the chimeric transcript between the exon 14 of *NTRK3* gene and the exon 2 of *EML4* gene, found by next-generation sequencing.

case. In addition, immunohistochemical analyses were helpful in the differential diagnosis in that MPNST does not show diffuse S100 immunoreactivity (with very rare exceptions) while, unlike in our case, there is the loss of H3K27me3 expression.<sup>25</sup> The lack of previous local trauma allowed us to exclude the possibility of reparative keloid tissue. Dermatofibroma was excluded on the basis of CD34 and S100 expressions, as both markers are usually lacked in this lesion. In addition, although myoepithelioma may be usually S100-positive, it is also frequently positive for epithelial markers (CKs, EMA) and negative for CD34. Lastly, leiomyoma was ruled out on the basis of the absent expression of myogenic markers ( $\alpha$ -smooth muscle actin and desmin), while schwannoma was excluded because the tumor herein presented lacked a fibrous capsule, and it was diffusely positive for CD34.

Being aware of the existence of a novel group of spindle cell tumors exhibiting co-expression of S100 and CD34 and characterized by fusion events involving various tyrosine kinases, including *NTRK1-3*, *RAF1* and *BRAF*, molecular analyses were conducted to identify potential genetic alterations. NGS was performed using a DNA panel for the identification of point mutations, INDEL and copy number variations, and an RNA panel for the detection of gene fusions. The RNA sequencing revealed a quite unusual fusion rearrangement involving the exon 14 of *NTRK3* gene with the exon 2 of *EML4* gene (Figure 2D). Based on the morphological, immunohistochemical, and molecular features, a diagnosis of *NTRK3-EML4*-rearranged spindle cell tumor with co-expression of S100 and CD34 was rendered. The lesion focally reached the surgical resection margins but no residual tumor was found on the subsequent surgical enlargement. Neither distant metastatic disease nor other lesions were detected on full-

body computed tomography scans. Patient is now healthy with neither evidence of local recurrence nor distant metastases after a 48-month follow-up.

### DISCUSSION

*NTRK* rearrangements represent a recently described and relatively rare group of molecular drivers observed in a wide range of tumors from various anatomical locations, including the central nervous system, soft tissues and salivary glands.<sup>13</sup> These rearrangements mainly consist of fusions of *NTRK* gene family, most commonly *NTRK1*, *NTRK2* or *NTRK3*, with other partner genes.<sup>5,13</sup> This fusion results in the constitutive activation of the *NTRK* kinase domain, leading to the initiation of downstream signaling pathways, including the *MAPK* and *PI3K-AKT* pathways. This activation promotes cell proliferation and survival, leading to the recognition of *NTRK* fusion-positive tumors as distinct and potentially targetable entities.<sup>14</sup>

*NTRK* fusions are clinically actionable with first-generation *NTRK* tyrosine kinase inhibitors such as larotrectinib or entrectinib showing responses in both adult and pediatric patients with *NTRK* fusion-positive tumors.<sup>1</sup> The identification of *NTRK*-fused neoplasms often requires molecular profiling since histological features alone may not be specific. Techniques for identification include FISH, RT-PCR, and NGS.<sup>5</sup>

The *EML4* gene encodes a protein involved in microtubule stabilization, which is crucial for maintaining cell shape and function.<sup>15</sup> In oncology, the *EML4* gene has gained significant interest in that it undergoes genetic events in some tumors including nonsmall cell lung cancer (NSCLC), in which it is frequently fused with *ALK* gene.<sup>15</sup> *NTRK3-EML4* rearrangements are quite unusual and have been described in cases of NSCLC, cervicovaginal sarcomas, osseous

sarcomas, gangliogliomas, IFSs, congenital mesoblastic nephromas and dermatofibrosarcoma protuberans.<sup>15-19</sup>

In the 5th edition of the World Health Organization classification of soft tissue and bone tumors, *NTRK* fusion-related spindle cell tumors have been recognized as an emerging entity.<sup>20,21</sup> This category encompasses a spectrum of tumors exhibiting various morphologies, including bland-looking to high-grade tumors, with a variable clinical behavior. Tumors in this group include LPFNTs, spindle cell tumors with the co-expression of S100 and CD34 resembling MPNSTs, IFSs, adult-type fibrosarcoma, IFS-like lesions with related fusion kinases and spindle cell sarcomas with hemangiopericytoma or myopericytoma-like pattern.<sup>9,12</sup>

Histologically, most *NTRK*-fused mesenchymal tumors are characterized by a monotonous proliferation of bland-looking spindle cells with an infiltrative growth pattern and frequent dual expression of S100 and CD34, along with the lack of SOX-10 immunoreactivity.<sup>9,12</sup> Although this immunoprofile is helpful for the diagnosis, it should be emphasized that

it is not specific to *NTRK*-rearranged tumors, as overlapping morphological and immunohistochemical features can be detected in other tumors harboring alternative protein kinase fusions, particularly those involving *RET*, *RAF1*, and *BRAF*. The main differential diagnoses include primary/metastatic melanoma and MPNST. Both these tumors can be confidentially ruled out by means of immunohistochemistry. Apart from S100, melanoma typically exhibits diffuse and strong positivity for SOX10, Melan A, and HMB45 while MPNST frequently shows the complete loss of H3K27me3 expression.<sup>9,12,20-23</sup>

Although mesenchymal tumors with kinase rearrangements were initially described in superficial soft tissues, they have been reported in multiple deep anatomic locations, including thorax, gastrointestinal, and gynecologic tract.<sup>5,23</sup> We are aware of only 24 cases reported in the head and neck region to date, mostly in the form of single case reports or small case series<sup>8,12,24,26-29</sup> (Table I). The most frequent kinase genes involved in descending order were: *NTRK1* (13 cases), *NTRK3* (6 cases), *BRAF* (2 cases), *RET* (2

**Table I.** Clinico-pathologic and molecular features of the previously reported cases of mesenchymal tumors with kinase fusions in the head and neck region

| Authors                           | Cases (n) | Gender | Age  | Anatomic site                      | Morphology  | Gene fusion  | Fusion partner  | Outcome (follow-up time) |
|-----------------------------------|-----------|--------|------|------------------------------------|-------------|--------------|-----------------|--------------------------|
| Kao et al. <sup>8</sup>           | 2         | F      | 38 y | Scalp (dermis/subcutis)            | LPFNT       | <i>NTRK1</i> | NA              | NA                       |
|                                   |           | M      | 30 y | Scalp (dermis/subcutis)            | LPFNT       | <i>NTRK1</i> | NA              | NA                       |
| Kang et al. <sup>26</sup>         | 1         | M      | 3 y  | Forehead (dermis/subcutis)         | IFS-like    | <i>NTRK1</i> | <i>LMNA</i>     | NED (0.8 y)              |
| Agaram et al. <sup>27</sup>       | 1         | F      | 38 y | Scalp (dermis/subcutis)            | LPFNT       | <i>NTRK1</i> | NA              | NA                       |
| Suurmeijer et al. <sup>12</sup>   | 2         | M      | 4 y  | Mandible (bone/soft tissues)       | LPFNT       | <i>NTRK1</i> | <i>LMNA</i>     | NED (144 m)              |
|                                   |           | M      | 13 y | Maxilla (bone)                     | MPNST-like  | <i>NTRK1</i> | <i>LMNA</i>     | NED (648 m)              |
| Brčić et al. <sup>28</sup>        | 1         | M      | 50 y | Neck (subcutis)                    | LPFNT       | <i>NTRK1</i> | <i>LMNA</i>     | NED (20 m)               |
| Al-Ibraheemi et al. <sup>29</sup> | 2         | M      | 11 m | Neck (soft tissues)                | LPFNT       | <i>FNI</i>   | <i>EGF</i>      | NA                       |
|                                   |           | M      | 7 m  | Neck (soft tissues)                | LPFNT       | <i>RET</i>   | <i>VCL</i>      | NA                       |
| Xu et al. <sup>24</sup>           | 15        | F      | 0 m  | Face/neck (dermis/subcutis)        | IFS-like    | <i>NTRK3</i> | <i>ETV6</i>     | AWD (21 m)               |
|                                   |           | F      | 0 m  | Neck (soft tissues)                | IFS-like    | <i>NTRK3</i> | <i>ETV6</i>     | NA                       |
|                                   |           | M      | 0 m  | Submandibular (salivary gland)     | IFS-like    | <i>NTRK6</i> | <i>ETV6</i>     | NA                       |
|                                   |           | F      | 0 m  | Submandibular (salivary gland)     | IFS-like    | <i>MET</i>   | <i>RBPMS</i>    | NA                       |
|                                   |           | M      | 4 y  | Face (soft tissues)                | LPFNT       | <i>NTRK1</i> | <i>LMN4</i>     | NED (142 m)              |
|                                   |           | F      | 38 y | Mandible (bone/soft tissues)       | LPFNT       | <i>NTRK1</i> | NA              | NA                       |
|                                   |           | M      | 14 y | Scalp (dermis/subcutis)            | LPFNT       | <i>BRAF</i>  | NA              | NA                       |
|                                   |           | M      | 13 y | Frontal sinus (sinonasal tract)    | MPNST-like  | <i>NTRK1</i> | <i>LMNA</i>     | NED (648 m)              |
|                                   |           | M      | 18 y | Maxilla (bone)                     | MPNST-like  | <i>NTRK1</i> | <i>TPM3</i>     | NA                       |
|                                   |           | M      | 30 y | Nasal cavity (sinonasal tract)     | MPNST-like  | <i>NTRK1</i> | NA              | AWD (7 m)                |
|                                   |           | F      | 2 y  | Scalp (dermis/subcutis)            | Adult-type  | <i>NTRK1</i> | <i>TPR</i>      | NA                       |
|                                   |           | F      | 22 y | Scalp (dermis/subcutis)            | FS-like     | <i>BRAF</i>  | <i>KIAA1549</i> | NA                       |
|                                   |           | M      | 0 m  | Parotid (salivary gland)           | Adult-type  | FS-like      | <i>NTRK3</i>    | <i>ETV6</i>              |
| Present case                      | 1         | M      | 54 y | Skull base (bone and soft tissues) | IMT-like    | <i>RET</i>   | <i>KIF5B</i>    | NA                       |
|                                   |           |        |      | Skull base (bone)                  | Myxoma-like | <i>NTRK3</i> | NA              | NA                       |
|                                   |           |        |      | Oral cavity (upper gingiva)        | MPNST-like  |              |                 |                          |
|                                   |           |        |      | Oral cavity (upper gingiva)        | MPNST-like  | <i>NTRK3</i> | <i>EML4</i>     | NED (48 m)               |

M, male; F, female; m, months; y, years; NA, not available; NED, no evidence of disease; AWD, alive with disease; LPFNT, lipofibromatosis-like neural tumor; IFS, infantile fibrosarcoma; IMT, inflammatory myofibroblastic tumor; MPNST, malignant peripheral nerve sheath tumor; FS, fibrosarcoma.

cases) and *MET* (1 case).<sup>24</sup> Xu et al.<sup>24</sup> reported the largest cohort of cases in the head and neck region, including 15 patients with a median age of 13 years (age range: 0-63) with tumor located in all tissue plans: skin (4/15), bone (4/15), major salivary glands (2/15), sinonasal tract (2/15), mucosa of the upper gingival (1/15) and soft tissue of face or neck (2/15). The histologic spectrum ranged from tumors resembling MPNST, fibrosarcoma, LPFNT, IMT-like, and a previously unreported myxoma-like morphology.<sup>24</sup> Perivascular hyalinization and keloid/amyloid-like thick collagen bands were most commonly exhibited by MPNST-like and LPFNT-like lesions.<sup>24</sup> In addition to morphology, also histologic grade ranged from low-grade (13/15) to high-grade (2/15) tumors.<sup>24</sup> The data already present in the literature further reinforce the peculiarity of the present case, as it represents the second case of kinase-fused mesenchymal tumor arising from the oral mucosa and it exhibits a hitherto unreported gene fusion among these neoplasms, involving the exon 14 of *NTRK3* with the exon 2 of *EML4*. We would like to emphasize that, despite its bland morphology, we have classified the tumor herein presented as malignant based on the detection of focal nuclear pleomorphism and frank infiltration into the surrounding adipose and striated muscle tissues. Among the morphological subtypes described within the broad spectrum of this emerging entity, we believe that the present case could be placed among those exhibiting an MPNST-like morphology.

## CONCLUSIONS

In summary, the present case emphasizes that pathologists must be aware of mesenchymal tumors with kinase fusions, especially when dealing with a monotonous proliferation of bland-looking spindle cells with perivascular hyalinization and keloid-like thick collagen bands, fat infiltration (LPFNT-like), hypercellular solid areas (MPNST-like or fibrosarcoma-like) and co-expression of S100 and CD34. The recognition is crucial to promptly perform molecular analyses. It must be also kept in mind that these neoplasms may arise from both superficial and deep soft tissue and may also occur in unusual anatomic sites such as the oral cavity. Although there is still little evidence from the literature that anything beyond surgical removal and follow-up is necessary for the management of these tumors in the head and neck region, it may be crucial to distinguish them from other potential mimickers, as patients with kinase fusion-positive spindle cell tumors may potentially benefit from targeted therapies with kinase inhibitors, especially in the context of recurrent and/or metastatic disease.

## DECLARATION OF INTERESTS

The authors declare that they have no known competing financial interests or personal relationships that could have appeared to influence the work reported in this article.

## CREDIT AUTHORSHIP CONTRIBUTION STATEMENT

**Giuseppe Broggi:** Writing – review & editing, Writing – original draft, Formal analysis, Conceptualization. **Giulio Attanasio:** Writing – review & editing, Writing – original draft, Formal analysis, Conceptualization. **Antonio Bonanno:** Methodology. **Ignazio La Mantia:** Methodology. **Sabina Barresi:** Resources. **Rita Alaggio:** Validation. **Gaetano Magro:** Writing – review & editing, Validation.

## COMPLIANCE WITH ETHICAL STANDARDS

The study complied with the Ethical Principles for Medical Research Involving Human Subjects according to the World Medical Association Declaration of Helsinki; the noninterventional, retrospective nature of our study did not require any informed consent, even if written informed consent had been obtained from the patient before surgical procedures. The clinical information had been retrieved from the patients' medical records and pathology reports. Patients' initials or other personal identifiers did not appear in any images. Finally, all samples were anonymized before histology, immunohistochemistry, and molecular analysis; therefore, no further ethical approval was necessary to perform the study.

## FUNDING

This research received no external funding.

## RESEARCH DATA STATEMENT

All data generated in the present research are available from the corresponding author upon reasonable request.

## REFERENCES

1. Cocco E, Scaltriti M, Drilon A. NTRK fusion-positive cancers and TRK inhibitor therapy. *Nat Rev Clin Oncol*. 2018;12:731-747. <https://doi.org/10.1038/s41571-018-0113-0>.
2. Penel N, Lebellec L, Blay JY. Why will there never be a randomized trial for NTRK-rearranged tumors? *Ann Oncol*. 2023;34:626-628. <https://doi.org/10.1016/j.annonc.2023.04.001>.
3. Cuello M, García-Rivello H, Huamán-Garaicoa F, et al. Detection of NTRK gene fusions in solid tumors: recommendations from a Latin American group of oncologists and pathologists. *Future Oncol*. 2023;19:2669-2682. <https://doi.org/10.2217/fon-2023-0552>.
4. Patton A, Dermawan JK. Current updates in sarcoma biomarker discovery: emphasis on next-generation sequencing-based methods. *Pathology*. 2024;56:274-282. <https://doi.org/10.1016/j.pathol.2023.10.015>.

5. Weiss LM, Funari VA. NTRK fusions and Trk proteins: what are they and how to test for them. *Hum Pathol.* 2021;112:59-69. <https://doi.org/10.1016/j.humpath.2021.03.007>.
6. Davis JL, Al-Ibraheemi A, Ruzdzinski ER, Surrey LF. Mesenchymal neoplasms with NTRK and other kinase gene alterations. *Histopathology.* 2022;80:4-18. <https://doi.org/10.1111/his.14443>.
7. Nozzoli F, Lazar AJ, Castiglione F, et al. NTRK fusions detection in paediatric sarcomas to expand the morphological spectrum and clinical relevance of selected entities. *Pathol Oncol Res.* 2022;28:1610237. <https://doi.org/10.3389/pore.2022.1610237>.
8. Kao YC, Suurmeijer AJH, Argani P, et al. Soft tissue tumors characterized by a wide spectrum of kinase fusions share a lipofibromatosis-like neural tumor pattern. *Genes Chromosomes Cancer.* 2020;59:575-583. <https://doi.org/10.1002/gcc.22877>.
9. Suurmeijer AJ, Dickson BC, Swanson D, et al. The histologic spectrum of soft tissue spindle cell tumors with NTRK3 gene rearrangements. *Genes Chromosomes Cancer.* 2019;58:739-746. <https://doi.org/10.1002/gcc.22767>.
10. Punjabi LS, Sittampalam K. Expanding the spectrum of adult NTRK3-rearranged spindle cell neoplasms: a recurrent NTRK3-SQSTM1 fusion spindle cell tumor with deceptively bland morphology. *Am J Clin Pathol.* 2022;157:485-493. <https://doi.org/10.1093/ajcp/aqab167>.
11. Miettinen M, Felisiak-Golabek A, Luiña Contreras A, et al. New fusion sarcomas: histopathology and clinical significance of selected entities. *Hum Pathol.* 2019;86:57-65. <https://doi.org/10.1016/j.humpath.2018.12.006>. Epub 2019 Jan 8.
12. Suurmeijer AJH, Dickson BC, Swanson D, et al. A novel group of spindle cell tumors defined by S100 and CD34 co-expression shows recurrent fusions involving RAF1, BRAF, and NTRK1/2 genes. *Genes Chromosomes Cancer.* 2018;57:611-621. <https://doi.org/10.1002/gcc.22671>.
13. Marchetti A, Ferro B, Pasciuto MP, Zampacorta C, Buttitta F, D'Angelo E. NTRK gene fusions in solid tumors: agnostic relevance, prevalence and diagnostic strategies. *Pathologica.* 2022;114:199-216. <https://doi.org/10.32074/1591-951X-787>.
14. Zito Marino F, Pagliuca F, Ronchi A, et al. NTRK fusions, from the diagnostic algorithm to innovative treatment in the era of precision medicine. *Int J Mol Sci.* 2020;21:3718. <https://doi.org/10.3390/ijms21103718>.
15. Okamoto I, Nakagawa K. Echinoderm microtubule-associated protein-like 4-anaplastic lymphoma kinase-targeted therapy for advanced non-small cell lung cancer: molecular and clinical aspects. *Cancer Sci.* 2012;103:1391-1396. <https://doi.org/10.1111/j.1349-7006.2012.02327.x>.
16. Dang X, Xiang T, Zhao C, Tang H, Cui P. EML4-NTRK3 fusion cervical sarcoma: a case report and literature review. *Front Med (Lausanne).* 2022;9:832376. <https://doi.org/10.3389/fmed.2022.832376>.
17. Church AJ, Calicchio ML, Nardi V, et al. Recurrent EML4-NTRK3 fusions in infantile fibrosarcoma and congenital mesoblastic nephroma suggest a revised testing strategy. *Mod Pathol.* 2018;31:463-473. <https://doi.org/10.1038/modpathol.2017.127>.
18. Rubino S, Lynes J, McBride P, et al. NTRK3 gene fusion in an adult ganglioglioma: illustrative case. *J Neurosurg Case Lessons.* 2022;3:CASE21645. <https://doi.org/10.3171/CASE21645>.
19. Olson N, Rouhi O, Zhang L, et al. A novel case of an aggressive superficial spindle cell sarcoma in an adult resembling fibrosarcomatous dermatofibrosarcoma protuberans and harboring an EML4-NTRK3 fusion. *J Cutan Pathol.* 2018;45:933-939. <https://doi.org/10.1111/cup.13348>.
20. Sbaraglia M, Bellan E, Dei Tos AP. The 2020 WHO classification of soft tissue tumours: news and perspectives. *Pathologica.* 2021;113:70-84. <https://doi.org/10.32074/1591-951X-213>.
21. Choi JH, Ro JY. The 2020 WHO classification of tumors of soft tissue: selected changes and new entities. *Adv Anat Pathol.* 2021;28:44-58. <https://doi.org/10.1097/PAP.0000000000000284>.
22. Palla B, Su A, Binder S, Dry S. SOX10 expression distinguishes desmoplastic melanoma from its histologic mimics. *Am J Dermatopathol.* 2013;35:576-581. <https://doi.org/10.1097/DAD.0-b013e31827a0b98>.
23. Antonescu CR. Emerging soft tissue tumors with kinase fusions: an overview of the recent literature with an emphasis on diagnostic criteria. *Genes Chromosomes Cancer.* 2020;59:437-444. <https://doi.org/10.1002/gcc.22846>.
24. Xu B, Suurmeijer AJH, Agaram NP, Antonescu CR. Head and neck mesenchymal tumors with kinase fusions: a report of 15 cases with emphasis on wide anatomic distribution and diverse histologic appearance. *Am J Surg Pathol.* 2023;47:248-258. <https://doi.org/10.1097/PAS.0000000000001982>.
25. Magro G, Broggi G, Angelico G, et al. Practical approach to histological diagnosis of peripheral nerve sheath tumors: an update. *Diagnostics (Basel).* 2022;12:1463. <https://doi.org/10.3390/diagnostics12061463>.
26. Kang J, Park JW, Won JK, et al. Clinicopathological findings of pediatric NTRK fusion mesenchymal tumors. *Diagn Pathol.* 2020;15:114. <https://doi.org/10.1186/s13000-020-01031-w>.
27. Agaram NP, Zhang L, Sung YS, et al. Recurrent NTRK1 gene fusions define a novel subset of locally aggressive lipofibromatosis-like neural tumors. *Am J Surg Pathol.* 2016;40:1407-1416. <https://doi.org/10.1097/PAS.0000000000000675>.
28. Brčić I, Godschachner TM, Bergovec M, et al. Broadening the spectrum of NTRK rearranged mesenchymal tumors and usefulness of pan-TRK immunohistochemistry for identification of NTRK fusions. *Mod Pathol.* 2021;34:396-407. <https://doi.org/10.1038/s41379-020-00657-x>.
29. Al-Ibraheemi A, Folpe AL, Perez-Atayde AR, et al. Aberrant receptor tyrosine kinase signaling in lipofibromatosis: a clinicopathological and molecular genetic study of 20 cases. *Mod Pathol.* 2019;32:423-434. <https://doi.org/10.1038/s41379-018-0150-3>.